Magnetoelastic coupling in the frustrated antiferromagnetic triangular lattice $CuMnO_2$

C. Vecchini,[1,2] M. Poienar,[3] F. Damay,[4] O. Adamopoulos,[2,5] A. Daoud-Aladine,[1] A. Lappas,[2] J. M. Perez-Mato,[6] L. C. Chapon,[1] and C. Martin[3]

[1]*ISIS Facility, Rutherford Appleton Laboratory, STFC, Chilton, Didcot OX11 0QX, United Kingdom*

[2]*Institute of Electronic Structure and Laser, Foundation for Research and Technology-Hellas, Vassilika Vouton, Heraklion, 711 10 Crete, Greece*

[3]*Laboratoire CRISMAT, ENSICAEN, UMR 6508 CNRS, 6 Boulevard du Marechal Juin, 14050 Caen Cedex, France*

[4]*Laboratoire Leon Brillouin, CEA-CNRS, UMR 12, CEA-Saclay, 91191 Gif-sur-Yvette Cedex, France*

[5]*Department of Chemistry, University of Crete, Voutes, 710 03 Heraklion, Greece*

[6]*Departamento de Fisica de la Materia Condensada, Facultad de Ciencia y Tecnologia, Universidad del Pais Vasco (UPV)-EHU, Apdo. 644, 48080 Bilbao, Spain*

(Received 22 April 2010; published 2 September 2010)

The magnetic ordering transition coupled to a structural transition in the anisotropic triangular lattice $CuMnO_2$ is investigated by high-resolution neutron powder diffraction. Temperature dependence of the magnetic order parameter and relevant structural quantities, such as cell constants and atomic positions, and analysis of the Landau potential show that there is a unique critical temperature, as well as that the primary order parameter is magnetic. The structural phase transition, necessary to lift the magnetic degeneracy, is improper ferroelastic with a linear-quadratic coupling between strain and magnetization density.

DOI: 10.1103/PhysRevB.82.094404 PACS number(s): 75.50.Ee, 75.30.Gw, 75.85.+t, 62.20.D−

I. INTRODUCTION

Triangular magnetic lattices with anisotropic antiferromagnetic (AFM) exchange interactions have attracted considerable interest to date since several strongly correlated electron systems, including certain superconductors,[1] possess a transition-metal framework that maps into this specific frustrated topology. Particular attention has been paid recently to systems with an exchange integral along one of the triangular direction (J_2) and two equivalent integrals in the other two (J_1), equivalent to square lattices with a single nearest-neighbor (diagonal) interaction.[2,3] While for classical Heisenberg spins the ground state is ordered with a spiral modulation for $\alpha=\frac{J_2}{J_1}>0.5$,[4,5] in the presence of strong single-ion anisotropy or Ising spins, the ground state is macroscopically degenerate: the magnetic configuration is AFM along each of the "J_2" chains but the total exchange energy is invariant by reversing the direction of all spins in any given chain.[6,7] The nature of the ground state strongly depends on perturbations that will lift the frustration such as long-range interactions, coupling to nonmagnetic degrees of freedom, or quantum fluctuations.[8]

Triangular lattices are realized in a number of quasi-two-dimensional compounds such as AMO_2 (A=Li, Na, K, Cu, Ag, and M=transition metal) or A_2MO_2 (A=Ag) all formed by MO_2 compact layers with M^{3+} ions in edge-sharing octahedral coordination.[9] In the case of Mn^{3+} in $t_{2g}^3eg^1$ electronic configuration induces a cooperative ferro-orbital ordering above room temperature and the associated structural distortion (monoclinic space group $C2/m$) promoting elongated Mn-O bonds along the axis of the dz^2 orbitals, establishes an anisotropic triangular lattice. The single-ion anisotropy term plays an important role since the Mn spins lie systematically along the axis of the dz^2 orbitals. The magnetic exchange, dominated by direct overlap of d orbitals (nearly 90° Mn-O-Mn bonds),[10] is much stronger along the shortest Mn-Mn triangular side ($J_2 \gg J_1$),[11] positioning these systems in the frustrated part of the phase diagram.

Despite displaying isostructural MnO_2 layers and identical in-plane magnetic configurations, the Na, Ag, and Cu analogs promote different ground states: for $NaMnO_2$, the magnetic excitation is gapped,[12] and the dynamics are well-explained by quasi-one-dimensional magnetic excitations, whereas for Ag_2MnO_2 the excitations are gapless.[13] The Na and more recently the Cu systems,[14] show a structural phase transition coincidental with a long-range magnetic ordering transition, but the magnetic order in the Ag system is short range and with no apparent structural distortion.

In this paper, we present a detailed study of the structural phase transition below the AFM order (T_N=65 K) in $CuMnO_2$ by high-resolution neutron powder diffraction. The structural phase transition is more pronounced than for $NaMnO_2$,[15] and the high-resolution data enables to follow critical parameters as a function of temperature,[16] an information not accessible in our previous study.[14] We prove unambiguously that the magnetic phase transition is *improper ferroelastic* in nature. The stronger magnetoelastic coupling in $CuMnO_2$ is inferred to the linear coordination of Cu to O that allows the development of shear strains at low-energy costs. It follows that the A-site cation, strongly affecting the elastic properties, should act as an excellent control lever for tuning the magnetoelastic coupling and ultimately the magnetic ground state of the AMO_2 and A_2MnO_2 compounds.

II. EXPERIMENTAL

5g of $CuMnO_2$ were prepared by high-temperature solid state reaction. Stoichiometric amounts of CuO and MnO powders were weighted, crushed, and pressed in the form of bars, which were then put inside a platinum crucible, introduced in an evacuated ampoule, and heated up to 950° for 12 h. The sample quality was checked by room temperature

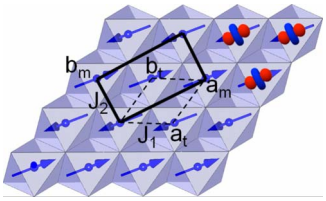

FIG. 1. (Color online) Crystal structure of $CuMnO_2$ projected in the *ab* plane. Mn ions, their associated ordered moments in the AFM state and MnO_6 octahedra are shown as spheres, arrows, and polyhedra, respectively. The monoclinic unit cell in the paramagnetic state and triclinic cell in the ordered state are shown as black solid and dashed lines, respectively. The ferro-orbital ordering of the Mn dz^2 is also represented.

x-ray diffraction, confirming a single-phase, well-crystallized, powder corresponding to the crednerite structure.[17–19] High-resolution neutron-powder-diffraction measurements in the temperature range 2–300 K were performed on the HRPD (High Resolution Powder Diffractometer) at the ISIS facility at the Rutherford Appleton Laboratory, U.K. The sample was placed in a slab can with vanadium windows. Rietveld refinements of the neutron data, including nuclear and magnetic phases, were performed with the program FULLPROF.[20] Symmetry analysis was performed using complete irreducible representations calculated using the induction procedure described in Ref. 21 and checked for consistency with the web-based applications of the Bilbao crystallographic server.[22] Susceptibility measurements were performed on a standard superconducting quantum interference devices both in zero field and in field cooled mode with an applied field of 3000 Oe in the temperature range $T=5-350$ K.

III. RESULT

The room-temperature monoclinic structure of $CuMnO_2$ refined from high-resolution data is in agreement with that recently reported by Damay *et al.*[14] and show the typical crednerite structure,[17] space group $C2/m$. The Mn^{3+} ions occupy the $2a$ Wyckoff site, (0,0,0) which is octahedrally coordinated by oxygens in the $4i$ site, [0.40715(8), 0, 0.17884(7)]. $Mn^{3+}O_6$ octahedra share edges to form $[MnO_2]_\infty$ layers in the *ab* plane (Fig. 1). Mn ions are arranged in planes of isosceles triangles with a short Mn-Mn bond length directed along the *b* axis [2.883(1) Å] and longer Mn-Mn bonds [3.148(1) Å] in the other two triangular directions ([110] and $[\bar{1}10]$), as shown in Fig. 1. The MnO_2 layers are linked by nonmagnetic Cu^+ ions [Wyckoff site $2d$ (0, 0.5, 0.5)] and are linearly coordinated by two oxygen ions forming O-Cu-O dumbbells perpendicular to the *ab* plane. Figure 3(a) shows the measured thermal variation in the first derivative of the inverse magnetic susceptibility for $CuMnO_2$. Due to the presence of short-range correlations well above T_N, there is no evidence of the three-dimensional (3D) magnetic order in the susceptibility which displays a broad maximum. However, an accident is observed in the first derivative of χ^{-1} that indicates the onset of 3D order below 65 K, in agreement with the presence of magnetic

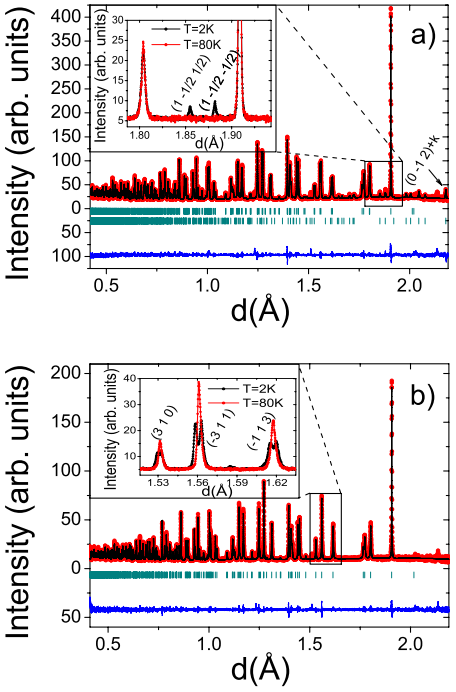

FIG. 2. (Color online) Rietveld refinements of the neutron diffractograms collected for $CuMnO_2$ (a) in the magnetically ordered state at 2 K [lattice parameters in triclinic space group: $a=3.14207(2)$ Å, $b=3.13425(2)$ Å, $c=5.89192(3)$ Å, $\alpha=102.2899°(7)$, $\beta=102.4245°(7)$, and $\gamma=54.6179°(4)$] and (b) in the paramagnetic regime at 80 K [lattice parameters in monoclinic space group: $a=5.57969(4)$ Å, $b=2.87972(2)$ Å, $c=5.89125(4)$ Å, and $\beta=103.9355°(7)$]. The circle points, solid lines and tick marks represent, respectively, the data, the result of the Rietveld refinement and the positions of the Bragg peaks. The solid lines at the bottom of each graph, represents the difference curve between experiment and fit. The top and bottom inset shows, respectively, the presence of magnetic Bragg peaks and splitting of some nuclear reflections below T_N.

Bragg scattering below this temperature. It is clear from Fig. 3(a) that the magnetic transition at $T_N=65$ K coincides with the structural phase transition to triclinic symmetry.[14] We note that at lower temperature, a tiny ferromagnetic contribution is observed due to the presence of small quantity of Mn_3O_4 (evaluated at 0.19% molar fraction from x-ray measurements not reported here) which produces a discontinuity in the differential inverse magnetic susceptibility [Fig. 3(a)]. In our previous work, the evidence for the structural phase transition was deducted from the offset at T_N of certain Bragg peaks at low-momentum transfer (Q). In the present study, the high resolution of the HRPD instrument allows to clearly resolve the splitting of several classes of nuclear reflections below T_N as shown in Fig. 2(b) for the peaks (3 1 0), $(\bar{3}11)$, and $(\bar{1}13)$, providing further insight about the structural changes. It confirms the triclinic (T) cell (space group $P\bar{1}$) below T_N, related to the monoclinic (M) cell (space group $C2/m$) by the transformation: $a_t=\frac{1}{2}a_m-\frac{1}{2}b_m$, $b_t=\frac{1}{2}a_m+\frac{1}{2}b_m$, $c_t=c_m$. Rietveld refinements of the neutron data above and below T_N are shown in Figs. 2(b) and 2(a), respectively. The lattice parameters have been extracted from

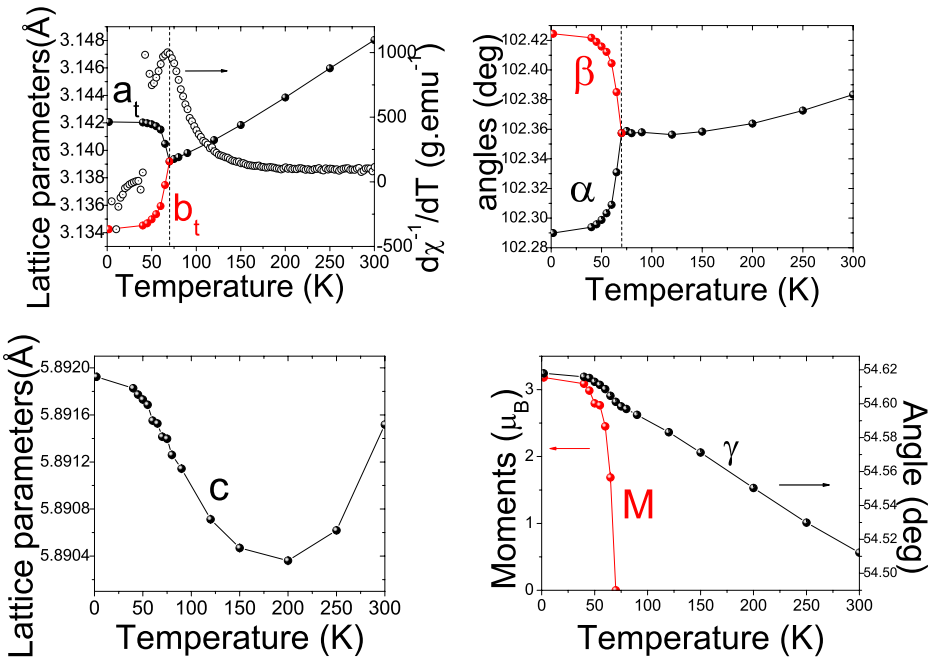

FIG. 3. (Color online) Temperature dependence of lattice parameters for $CuMnO_2$ extracted from Rietveld refinements of neutron data in the low temperature $P\bar{1}$ space group. Experimental points are displayed as circles and lines are guide to the eye. The vertical line marks the critical temperature. The differential of the zero-field-cooled inverse susceptibility data in the temperature range 5–300 K at an applied magnetic field of 3000 Oe is displayed in the first panel together with the splitting of the lattice parameters.

the Rietveld refinements of neutron diffractograms collected at several temperatures. Data have been refined using the monoclinic space group $C2/m$ above T_N=65 K and triclinic symmetry $P\bar{1}$ below T_N. The temperature dependences of all lattice parameters are displayed in Fig. 3. The symmetry lowering results in a splitting of the in plane parameters (a_t and b_t in one hand and α and β on the other). We also note a very small increase in the γ parameter below 65 K. The transition is second order with a continuous change in the cell angles through the phase transition. The change in Laue class $2/m \rightarrow \bar{1}$ indicates that two components of the strain tensor, $e_4=\epsilon_{yz}$ and $e_6=\epsilon_{xy}$, are active at the transition. They can be evaluated from the precise values of lattice parameters obtained in the entire temperature range (Fig. 3): the variation in all cell parameters where fitted above T_N using Einstein models that were extrapolated below T_N to provide baseline values for an "undistorted" monoclinic cell.[23] The components of the strain tensor were calculated using the cell parameters in the triclinic phase and the baseline values using the equations given in.[24,25] The temperature dependence of e_4 and e_6, presented in Fig. 4 follows a critical behavior with saturation values of the strain components around 0.1%, typical of improper ferroelastics.[26] All other strain components are extremely small and do not seem to follow a critical behavior. The other structural secondary order parameter of the transition is the displacement mode of the oxygen, constrained in the $(x,0,z)$ positions above T_N and in general position below the transition. The amplitude of the mode along the y direction, not shown, is clearly nonnull (oxygen position at T=2 K: [0.40668(8), 0.4078(3), 0.17888(6)]) although it is difficult to extract a quantitative value due to the small displacements involved.

In order to describe fully the transition, one needs to consider the magnetic order parameter which becomes also critical at the same temperature (Fig. 3). The magnetic wave vector is $\mathbf{k}=(\frac{1}{2},\frac{1}{2},\frac{1}{2})$ with respect to the C-centered monoclinic cell [$\mathbf{k}=(0,\frac{1}{2},\frac{1}{2})$ in $P\bar{1}$] and the moments points along the direction of the dz^2 orbitals. The magnetic ordering corresponds to a transition from the paramagnetic point group $2/m1'$ to the point group $\bar{1}1'$. According to the previous study of Damay *et al.*, the direction of the magnetic moment does no vary with temperature, implying that the magnetic order parameter can be directly evaluated from the square

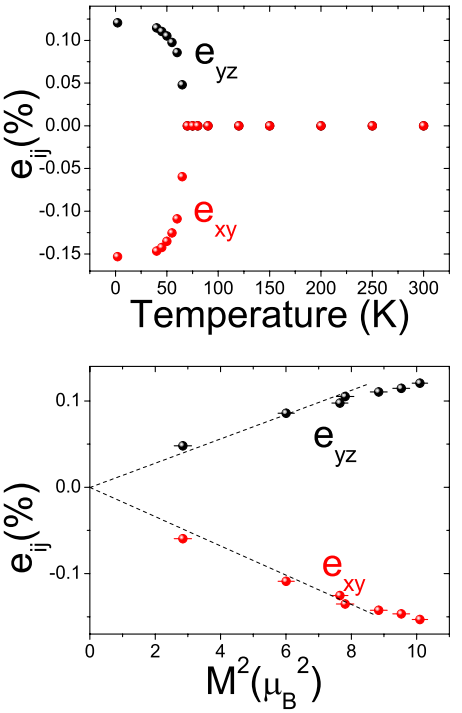

FIG. 4. (Color online) (a) Temperature dependence of the strain parameters e_{yz} and e_{xy}. (b) Linear-quadratic dependence of the active strain components below T_N with respect to the magnetic order parameter.

TABLE I. Irreducible representation L_1^+ and GM_2^+ for the space group $C2/m1'$. Symmetry operations are listed in the Seitz notation. For L_1^+, the matrices act on the two-dimensional space formed by the magnetic order parameter (η_1, η_2) related with the two arms of the star. Time-reversal operation is noted $1'$. The second line shows the irreducible representation GM_2^+ at the center of the zone $(k=0)$.

	$\{2_y\|000\}$	$\{\bar{1}\|000\}$	$\{m_{xz}\|000\}$	$\{1\|100\}$ $\{1\|010\}$ $\{1\|001\}$	$\{1\|\frac{1}{2}\frac{1}{2}0\}$
				$1'$	
L_1^+	$\begin{pmatrix} 0 & 1 \\ 1 & 0 \end{pmatrix}$	$\begin{pmatrix} 1 & 0 \\ 0 & 1 \end{pmatrix}$	$\begin{pmatrix} 0 & 1 \\ 1 & 0 \end{pmatrix}$	$\begin{pmatrix} -1 & 0 \\ 0 & -1 \end{pmatrix}$	$\begin{pmatrix} -1 & 0 \\ 0 & 1 \end{pmatrix}$
GM_2^+	-1	1	-1	1	1

root of the integrated intensity of magnetic superlattice reflections. On the HRPD data, the most intense magnetic Bragg peak accessible in the limited Q range is the $(0-1\ 2)+\mathbf{k}$ $(d=2.178$ Å) as shown in Fig. 2(a). The temperature dependence of the magnetic moments is shown in Fig. 3.

Using a Landau expansion of the thermodynamic potential and the measured temperature dependence of the magnetic and elastic order parameters, one can rigorously prove that the phase transition is driven by magnetic ordering. Since the star of $\mathbf{k}$ is made of the two vectors $\mathbf{k}_1=(\frac{1}{2},\frac{1}{2},\frac{1}{2})$ and $\mathbf{k}_2=(-\frac{1}{2},\frac{1}{2},-\frac{1}{2})$, one needs to consider the complete irreducible representation L_1^+ (Miller-Love notation[27]) acting on the two-dimensional magnetic order parameter (η_1, η_2). The matrices representative of L_1^+ for the paramagnetic $C2/m1'$ group are shown in Table I, together with the irreducible representation GM_2^+ of the point group $2/m$, upon which the two active components of the strain e_4 and e_6 and the displacive mode of the oxygen atoms along y transform. The magnetoelastic coupling invariant of lowest degree that can be formed is $(\eta_1^2-\eta_2^2)e_i$, where $i=4$ or $i=6$. The thermodynamic potential including the magnetic order parameter for a single domain η, magnetoelastic and magnetostructural coupling terms can be written

$$F = F_0 + \frac{\alpha}{2}\eta^2 + \frac{\beta}{4}\eta^4 + (\gamma_4 e_4 + \gamma_6 e_6)\eta^2 + \frac{\delta}{2}Q_y\eta^2 + \frac{1}{2}\omega^2 Q_y^2 + \frac{1}{2}\sum_{ij} C_{ij}e_i e_j + \cdots,$$

where the $C_{\alpha\beta}(\alpha,\beta=1,\ldots,6)$ represent the elastic constant of the high-temperature phase and the strain components are defined using the Voigt notation[28] and Q_y is the mode associated to the oxygen atom. The last term represents the elastic energy and run over 13 terms in monoclinic symmetry. The equations of state show that the equilibrium value of the strain component $e_i(i=4,6)$ below T_N depends quadratically on the magnetic order parameter, following the equation $e_i = -\frac{\gamma_i}{C_{ii}}\eta^2$. This condition is realized, as evidenced by plotting the component e_4 and e_6 determined experimentally against the magnetic intensity (proportional to η^2) showing a linear relation between the two quantities close to T_N (Fig. 4). At lower temperature, the deviation from linearity is due to the contributions to higher degree invariants. Also, the two domains corresponding to k_1 and k_2 have, respectively, opposite signs for the strain coefficients e_{xy} and e_{yz}. The transition in $CuMnO_2$ can therefore be classified as improper ferroelastic and the material displays *spin-driven* ferroelasticity by analogy to the recently discussed spin-driven ferroelectric transition (Ref. 29 and references therein) in frustrated magnets. The coupling between magnetic and elastic degrees of freedom indicates that a single antiferromagnetic domain (corresponding to either $\mathbf{k}_1$ or $\mathbf{k}_2$) can be stabilized by application of an external stress below T_N or if the material is cooled in a strain field. It also appears that the magnitude of the induced strain, based on comparison with available data on the $NaMnO_2$ and Ag_2MnO_2 analogs,[13,16] varies greatly depending on the nature of the A-site cation and its coordination. In the present system, the Cu is linearly coordinated to the oxygen, and the atomic positions show that the O-Cu-O angle remain unaffected at the transition. Indeed the Cu is located on an inversion symmetry point and the O-$\widehat{\text{Cu}}$-O angle remains 180° below T_N. It also means that a relatively large structural modification between adjacent layers does not induce a major change in elastic energy compared to the other systems. It would be valuable to attempt partial substitutions on the A site in order to be able to fine tune the balance between elastic energy and magnetic energy and systematically study the transition from a disordered magnetic state to long-range order in these frustrated systems. Our experiment also suggests that external pressure at low temperature could drastically affect the magnetoelastic coupling.

ACKNOWLEDGMENTS

A.L. acknowledges partial support from the European Commission ("Construction of New Infrastructures," ISIS Target Station II, Contract No. 011723), and the EU access to research infrastructures program of ISIS (Project No.: HPRI-CT-2001-00116).

[1] J. Merino, R. H. McKenzie, J. B. Marston, and C. H. Chung, J. Phys.: Condens. Matter **11**, 2965 (1999).
[2] P. Chandra, P. Coleman, and A. I. Larkin, Phys. Rev. Lett. **64**, 88 (1990).
[3] F. Becca and F. Mila, Phys. Rev. Lett. **89**, 037204 (2002).
[4] Z. Weihong, R. H. McKenzie, and R. R. P. Singh, Phys. Rev. B **59**, 14367 (1999).
[5] S. R. White and I. Affleck, Phys. Rev. B **54**, 9862 (1996).
[6] T. P. Eggarter, Phys. Rev. B **12**, 1933 (1975).
[7] Y. Tanaka and N. Uryû, J. Phys. Soc. Jpn. **44**, 1091 (1978).
[8] M. J. Harris, S. T. Bramwell, D. F. McMorrow, T. Zeiske, and K. W. Godfrey, Phys. Rev. Lett. **79**, 2554 (1997).
[9] T. A. Hewston and B. L. Chamberland, J. Phys. Chem. Solids **48**, 97 (1987).
[10] J. B. Goodenough, A. Wold, R. J. Arnott, and N. Menyuk, Phys. Rev. **124**, 373 (1961).
[11] A. Zorko, S. E. Shawish, D. Arcon, Z. Jaglicic, A. Lappas, H. van Tol, and L. C. Brunel, Phys. Rev. B **77**, 024412 (2008).
[12] C. Stock, L. C. Chapon, O. Adamopoulos, A. Lappas, M. Giot, J. Taylor, M. A. Green, C. M. Brown, and P. G. Radaelli, Phys. Rev. Lett. **103**, 077202 (2009).
[13] S. Ji, J. H. Kim, Y. Qiu, M. Matsuda, H. Yoshida, Z. Hiroi, M. A. Green, T. Ziman, and S. H. Lee, arXiv:0907.3157v1 (unpublished).
[14] F. Damay, M. Poienar, C. Martin, A. Maignan, J. Rodriguez-Carvajal, G. André, and J. P. Doumerc, Phys. Rev. B **80**, 094410 (2009).
[15] M. Jansen and R. Hoppe, Z. Anorg. Allg. Chem. **399**, 163 (1973).
[16] M. Giot, L. C. Chapon, J. Androulakis, M. A. Green, P. G. Radaelli, and A. Lappas, Phys. Rev. Lett. **99**, 247211 (2007).
[17] I. D. Kondrashev, Sov. Phys. Crystallogr. **3**, 703 (1959).
[18] Y. Bessekhouad, Y. Gabes, A. Bouguelia, and M. Trari, J. Mater. Sci. **42**, 6469 (2007).
[19] J. Töpfer, M. Trari, P. Gravereau, J. P. Chaminade, and J. P. Doumerc, Z. Kristallogr. **210**, 184 (1995).
[20] J. Rodriguez-Carvajal, Physica B **192**, 55 (1993).
[21] O. Kovalev, in *Representation of the Crystallographic Space Groups*, edited by H. Stokes and D. Hatch (Gordon and Breach, New York, 1993).
[22] M. I. Aroyo, A. Kirov, C. Capillas, J. M. Perez-Mato, and H. Wondratschek, Acta Crystallogr., Sect. A: Found. Crystallogr. **62**, 115 (2006).
[23] A. Einstein, Ann. Phys. **22**, 180 (1907).
[24] J. L. Schlenker, G. V. Gibbs, and M. B. J. Boisen, Acta Crystallogr., Sect. A: Cryst. Phys., Diffr., Theor. Gen. Crystallogr. **34**, 52 (1978).
[25] E. K. Salje, *Phase Transitions in Ferroelastic and Co-elastic Crystals* (Cambridge University Press, Cambridge, 1993).
[26] R. J. Reeder, S. A. T. Redfern, and E. Salje, Phys. Chem. Miner. **15**, 605 (1988).
[27] S. C. Miller and W. F. Love, *Tables of Irreducible Representations of Space Groups and Co-Representations of Magnetic Space Groups* (Pruett Press, Boulder, CO, 1967).
[28] W. Voigt, *Lehrbuch der Kristallphysik* (Teubner, Leipzig, Berlin, 1928).
[29] W. Eerenstein, N. D. Mathur, and J. F. Scott, Nature (London) **442**, 759 (2006).